Minicircle production and delivery to human mesenchymal stem/stromal cells for angiogenesis stimulation

Liliana Isabel Casimiro Brito, MSc Biotechnology

IST, Lisbon, Portugal

The potential of mesenchymal stem cells (MSC) has attracted much attention in regenerative medicine due to their unique biological properties. MSC transplantation associated to angiogenic gene therapy is a promising strategy of treatment for cardiovascular diseases (CVD). Although MSC intrinsically produce vascular endothelial growth factor (VEGF), which is a protein involved in the angiogenesis stimulation, its overexpression can enhance their therapeutic properties in cardiac regeneration. Regarding gene delivery methods, non-viral systems are a priority in gene therapy field. As an alternative to conventional plasmid DNA, in this master thesis the minicircle technology was explored. VEGF-GFP encoding minicircles were produced by *Escherichia coli* BW2P *in vivo* recombination induced in the mid-end exponential phase which led to recombination efficiencies over 90%. Regarding the purification, minicircle population represents roughly 15% of the sample and its recovery from anion exchange (AEC) and hydrophobic interaction (HIC) chromatography was 50-67% and 40-46% respectively and must be improved. MSC transfected with minicircles attained a maximum of 301±8% of GFP-expressing cells, considering the CMV and mCMV+hEF1αCpG free promoters and no significant difference was observed in comparison with the pVAX-VEGF-GFP. However, higher survival of MC MSC transfected cells and ELISA results showed an at least 1.3-fold higher VEGF concentration than pVAX-VEGF-GFP after 7 days of transfection. The hEf1α and hEf1αCpG free promoters showed low levels of expression. This work showed that minicircles hold potential to enhance MSC therapy efficacy for the treatment of CVD through angiogenesis.

Keywords: Mesenchymal stem cells, angiogenesis, cardiovascular diseases, non-viral gene therapy, minicircle

1. Introduction

Among non communicable diseases (NCD), the cardiovascular diseases, which include heart and blood vessels diseases, are the major cause of NCD deaths [1]. For the successful cardiac tissue regeneration as well as the treatment of ischemic cardiac tissue, a controlled angiogenesis is required. Using limb or myocardial ischemic models, differentiated cells, such as hematopoietic cells and myoblasts, have been shown to induce vessel formation by expressing angiogenic factors [2, 3]. However, their clinical application is hindered by the difficulty in obtaining a large cell number, their lack of ability to expand *in vitro* and poor engraftment efficiency to target tissue sites [2]. Within stem cells, mesenchymal stem cells (MSC) showed their regenerative potential since they can be readily and easily isolated and *ex vivo* expanded from a wide range of tissues, are capable of undergoing multilineage differentiation, show hypoimmunogenicity and immunomodulatory properties, have migration behaviour to injury sites, trophic ability and no ethical limitations[4, 5]. On the other hand, the MSC regenerative capacity is limited partly by the insufficient expression of angiogenic factors and low survival rate of the transplanted cells [2,6]. As a result, a combination of cell and angiogenic gene therapies would improve this poor viability [7,8]. For example, transplant of MSC modified with an Adeno-associated viral vector to overexpress VEGF under hypoxic conditions increased MSC cell survival, induced angiogenesis and improved overall heart function [6]. However gene transfer via viral systems remains the most prevalent choice in clinical trials [9], gene therapy biosafety using non-viral vectors can be achieved if the positive traits of viruses are included and genotoxicity negative traits are eliminated.

Although MSC are less accessible to transfection using non-viral vectors, from the current non-viral methods available, liposome carriers and electroporation-based gene transfer techniques were determined to be the most efficient [10,11]. An improved version of electroporation, namely microporation, used in this work, has shown promising results not only in transfection efficiency but also in terms of cell survival [12,13]. The success of gene delivery depends also on the DNA-based vector ability to overcome physical and metabolic barriers during trafficking to the cell nucleus and also on the regulation of the transgene expression [14]. Derived from conventional plasmid DNA (pDNA), supercoiled minimal expression cassettes were developed. Minicircles (MC) no longer contain antibiotic resistance markers, the bacterial origin of replication and other inflammatory sequences intrinsic to bacterial backbone of pDNA. Besides the low risk of immunogenic responses that MC present, a number of studies have demonstrated that MC vectors greatly increase the transgene expression in various *in vitro* and *in vivo* studies, in terms of high and persistent expression levels. Without integration into the host genome, these vectors also prevent unwanted genomic changes in the cells, demonstrating a great potential for the treatment of several diseases [15-18]. Regarding MC production technology, it is based on two steps: the recombination process and the purification methods. In *E.coli* strains, the MC are the result of an *in vivo* site-specific intramolecular recombination process from a parental plasmid (PP). The PP carries the transcription unit flanked by two recognition sites of a site-specific recombinase. The *in vivo* induction of the expression of the respective recombinase results in the excision of the interjacent DNA sequences, dividing the PP into two supercoiled molecules: a replicative miniplasmid (MP) carrying the undesired bacterial backbone sequences and a minicircle carrying the therapeutic expression unit [19]. The minicircle model system used in this work relies on ParA resolvase, a recombinase that is under transcription control of the arabinose inducible expression system pBAD/AraC [19]. MC purification is one of the major limiting steps of industrial MC production, hence new strategies have been developed over time. Chromatographic methods based on charge and affinity differences were already explored [19-22]. In this study, a different chromatographic method based on hydrophobic interaction was tested as an inexpensive and easily scalable alternative [23].

2. Materials and Methods

2.1. Plasmids construction

pMINILi plasmid (3987bp) is derived from the parental plasmid pMINI8 (4702bp)[19] by deletion of the P_{BAD}/*araC-parA* cassette (715bp) using a directed mutagenesis protocol with KOD Hot Start Master Mix (Novagen®) followed by AgeI enzymatic digestion and ligation with T4 ligase enzyme (3U/µL, Promega). pMINILi-CMV-VEGF-GFP plasmid (4563bp) was constructed by the insertion of VEGF gene fragment into the pMINILi double digested with EcoRI and KpnI restriction enzymes. The VEGF gene fragment was obtained by double digestion of the pVAX-VEGF-GFP (4273bp) with the same enzymes. pMINILi-mCMV+hEF1α(CpG free)-VEGF-GFP plasmid (4560bp) was constructed from pMINILi-CMV-VEGF-GFP by changing the CMV to the mCMV+hEF1α(CpG free) promoter. After purification of the pCpG free-mcs plasmid (3049bp) present in *E.coli* GT115, the promoter fragment (761bp) was obtained by digestion with PstI restriction enzyme. At the same time, pMINILi-CMV-VEGF-GFP was digested with the same enzyme and the two fragments were ligated. After a HindIII digestion, the provisional pMINILi-CMV-mCMV+hEF1α(CpG free)-VEGF-GFP plasmid (5234bp) was confirmed taking into account the correct orientation of the promoter. For the construction of pMINILi-mCMV+hEF1α (CpG free)-VEGF-GFP a final double digestion with NheI and MluI enzymes removed the original CMV promoter. Derived from the aforementioned pMINILi-CMV-mCMV+hEF1α(CpG free)-VEGF-GFP (5234bp), the pMINILi-hEF1α(CpG free)-VEGF-GFP (4125bp), was constructed by deletion of the original CMV promoter and the enhancer mCMV using a single SpeI restriction digestion. The expected plasmid constructions were confirmed by DNA sequencing of modified regions by Stabvida (Lisbon, Portugal).

2.2. Minicircles production

5mL of LB medium supplemented with kanamycin (30µg/mL) and 0.5% (w/v) glucose were inoculated with a loop of frozen *E.coli* BW2P from the specific cell banks and incubated overnight at 37ºC, 250 rpm. Next, an appropriate volume of the first seed culture was used to inoculate 30mL of LB media also supplemented with kanamycin (30µg/mL) and 0.5% (w/v) glucose up to an initial OD_{600nm} of 0.1. Before the inoculation, the specific culture volume was centrifuged at 6000g and then it was resuspended in fresh culture media. Afterwards, cultures were incubated at 37ºC and 250rpm until reaching an OD_{600nm} close to 2.5 (exponential phase). At that moment, an appropriate volume of seed culture was once again used to inoculate 250mL of LB medium supplemented only with kanamycin (30µg/mL) and to achieve an initial OD_{600nm} of 0.1. Cultures were then incubated at 37ºC and 250rpm. Monitoring the OD_{600nm} during the growth, in this study, recombination induction was performed at OD_{600nm} between 2.4 and 3.6. Also, the pH was checked whether the values were between 7.0 and 8.5. The recombination was induced by adding 0.01% (w/v) of 20% (w/v) L-(+)-arabinose (Merck Millipore) directly to the

medium and recombination was allowed to proceed for 2 or 5 hours. 2mL culture samples at the induction time and during induction (2h or 5h) were withdrawn hourly to allow recombination characterization on agarose gel electrophoresis. The final culture was centrifuged to obtain cell pellets that were stored at -20ºC for further purification. 2mL culture samples collected before and after recombination induction were used to isolate the respective pDNA. Specifically, purified plasmids relative to the final culture time were digested with SacII, a restriction enzyme with only one restriction site on the MP and, respectively, on the PP. After gel electrophoresis of the SacII restriction mixtures, the recombination efficiency was calculated on the basis of band intensities obtained with the ImageJ software (peak areas) and normalized for molar amounts using the following equation [19, 24]:

$$E_r(\%) = \left(1 - \frac{PP_{mol}}{MP_{mol}+PP_{mol}}\right) \times 100 \quad \text{(Equation 1)}$$

where E_r is the efficiency of recombination, PP_{mol} is the molar amount of parental plasmid and MP_{mol} is the molar amount of miniplasmid. The same protocol was performed for cell cultures in 500mL of LB medium.

2.3. Total pDNA purification

The cellular lysis and purification of the total pDNA was performed with Endotoxin-free Plasmid DNA Purification NucleoBond® XtraMidi hEF kit (Macherey-Nagel), according to the manufacturer protocol and also using half of the columns suggested. The concentration of purified pDNA solutions was assayed by spectrophotometry at 260nm (Nanodrop, Thermo Scientific, Waltham, MA) and DNA integrity was confirmed by DNA agarose gels stained with ethidium bromide(Et-Br). Volumetric yield (VY) was calculated by the following equation:$Volumetric\ Yield = \frac{Total\ mass\ pDNA}{Initial\ culture\ volume.}$ (Equation 2).

2.4. Minicircles purification

2.4.1. Anion Exchange Chromatography (AEC)

Total pDNA was digested by adding 1U of PvuII (50U/µL,Thermo Scientific™) per µg of recombinant products, 1X of the Buffer G and water to complete the total volume of 1mL. Enzymatic digestion was confirmed by DNA agarose gels stained with Et-Br. The Convective Interation Media Diethylaminoethyl monolith disk CIM®-DEAE (weak anion exchanger with diethylaminoethyl functional groups, 0.34mL, BIA Separations) was used in the AKTA Purifier 10 (GE Healthcare) system. The mobile phase consisted of the buffer A (20mM Tris-HCl, pH 9.0-9.2) and the buffer B (1M NaCl in 20mM Tris-HCl, pH 9.0-9.2). Sample volumes were injected manually in the column previously equilibrated. The mixture was separated firstly using a linear gradient at flow rate of 1mL/min (20-80% buffer B, gradient slope of 2%/min, 90CV(column volumes)) and then by a step gradient at flow rate of 1mL/min, which included four or five steps.. The salt concentrations corresponding to the top and end tail of the linear fragments peak (linear gradient) were used as a guide to set up the step gradient method. Considering the delay, meaning the time taken for gradient to reach column, the salt concentration to elute the impurities in step-gradient was adjusted as well as the salt concentration for MC elution. The absorbance of the eluate was continuously measured at the disk outlet at 260nm. Fractions of 0.1mL for minicircle and 0.2mL for impurities were collected in a 96-well plate and the significant peak fractions were visualized on gel electrophoresis.

2.4.2. Hydrophobic Interaction Chromatography (HIC)

Total pDNA was digested by adding 10µL of NB.bvCI DNA nickase enzyme (10U/µL, New England BioLabs®), 1X of the provided buffer and water to complete the total volume of 240µL. The Phenyl Sepharose 6 Fast Flow(High Sub) resin (10mL, GE Healthcare) was used in the AKTA Purifier 100 (GE Healthcare) system. The mobile phase included buffer A (2.2M $(NH_4)_2SO_4$) in 10mM Tris-HCl, pH 8.0) and buffer B (10mM Tris-HCl, pH 8.0). In this technique, DNA mixture was firstly conditioned in 2.5M of ammonium sulphate ($(NH_4)_2SO_4$) and then injected manually in the column previously equilibrated. The species were separated by a step gradient at a flow rate of 2mL/min, which included three steps: 17%B (4CV), 35%B (2CV) and 100%B (2CV). The absorbance of the eluate was continuously measured at the column outlet at 260nm and fractions of 1.5mL were collected in eppendorfs. The significant peak fractions were previously dialysed to eliminate the salt and afterwards, were visualized on gel electrophoresis.

2.4.3. Dialysis and Concentration

The MC pure fractions were collected and processed in Amicon® Ultra-2 30k (volume of 2mL and 30,000 NMWL cutoff, Merk Millipore), according to the respective protocol, in order to diafiltrate and concentrate the sample. MC samples were concentrated by Savant™ DNA120™ SpeedVac Concentrator (Thermo Scientific™) at low drying rate and their concentrations were determined by spectrophotometry at 260nm. MC recoveries for AEC and HIC were calculated by:

$$MC\ Recovery = \frac{m_{MC}}{m_{Load} \times \%MC\ peak\ area} \times 100 \quad \text{(Equation 3)}$$

2.5. BM MSC thawing and expansion

The different donor cryopreserved cells were thawed by submerging the cryovials in a 37ºC water bath and ressuspended in 4mL of Iscove's Modified Dulbecco's Medium (IMDM, Gibco®) supplemented with 20%FBS (Gibco®). After a centrifugation at 1250rpm for 7min, the pellet was ressuspended in Dulbecco's Modified Eagle Medium (DMEM, Gibco®) supplemented with 10%(v/v) MSC-qualified FBS (Hyclone®). Both media have 1%(v/v) of a mixture of antibiotics (Antibiotic-Antimycotic, 10,000 units/mL of penicillin, 10,000 µg/mL of streptomycin and 25 µg/mL of Fungizone® (amphotericin B) Antimycotic, Gibco®). The determination of total cell number and viabilities was estimated by the Trypan Blue (0.4%, Gibco®) dye exclusion method and a hemacytometer under an optical microscope (Olympus). According to the cell number, they were plated at cell culture flasks considering the more appropriate cell densities using DMEM+10%(v/v)MSC-

FBS+1%(v/v)AA medium and kept in an incubator at 37ºC, 19.5% O_2, 5% CO_2 and 98% humidity. The medium was replaced every 3-4 days. The cell passages were performed when 80% cell confluence was observed by microscope. This procedure first included a cell wash with Phosphate Buffered Saline buffer (PBS, Gibco®), followed by the cell detachment from the flask surface with Accutase solution (Sigma®) for 5min at 37ºC. Inactivation of the accutase was completed by adding IMDM+10%(v/v)FBS +1%(v/v)AA in a proportion of at least 2:1. Collected cells were concentrated by centrifugation and cell number and viability were accessed by the Trypan Blue dye exclusion method. At least one cell passage was done after thawing and before transfection experiment. The culture of CHO cells was carried out using the aforementioned conditions with exception of the fact that the medium contained a non-specific FBS and it was replaced every 2 days. Also, cell detachment from the flask surface was performed with Accutase solution but just for 2min at 37ºC.

2.6. BM MSC Microporation

For each transfection experiment using the Neon™ Transfection System, in one reaction, equivalent to a time point, $1.5x10^5$ BM MSC cells were ressuspended in ressuspension buffer (RB) supplied by the microporator manufacturer ($1.5x10^5$cells/10µL) and incubated with a specific amount of vector (pDNA or MC) followed by microporation. The microporation conditions used were: 1 pulse with 1000V of pulse voltage and 40ms of width. After microporation, each 10µL of cell suspension was introduced into an eppendorf containing the proper amount of Opti-MEM®I medium (Gibco®). 25µL of the previous mixture was transferred to a well, from 6-well plates, containing 3mL of DMEM medium with antibiotics and FBS. The cells were subsequently incubated under static conditions at 37ºC and a 5% CO_2-humidified atmosphere until the established time points (days 1, 4 and 7), after which they were collected for further analysis. Two different CHO cell microporation experiments were performed with the same transfection system but the microporation conditions recommended are 10 pulses with 1560V of pulse voltage and 5ms of width. There was only the collection of transfected cells for flow cytometric analysis on days 1 and 4. All transfection experiments were performed using cells at passages P5-P7 and in all experiments, non microporated cells were used as control.

2.6.1. Fluorescence Microscopy Imaging

Transfected and control cells were visualized using a fluorescence optical microscope Leica DMI3000B and Leica EL6000 compact light source (Leica Microsystems CMS GMbH) and digital images were obtained with a digital camera Nikon DXM 1200F. Fluorescence images were acquired with blue filter at 100X and 200X magnifications.

2.6.2. Flow cytometric analysis

For monitorization of the GFP-expressing cells on days 1,4 and 7, the transfected and control cells were first harvested using accutase, centrifuged and ressuspended in a cell fixative solution (1% paraformaldehyde (PFA, Sigma®)). Then, considering the acquisition of a minimum of 10 000 events, the number of GFP^+ cells was determined using BD FACSCalibur™ equipment (BD Biosciences) and statically evaluated by CellQuest™ Software (BD Biosciences). The level of GFP protein expression was given by mean fluorescence intensity (MFI) also measured during the flow cytometric procedure. Non-transfected cells were used to determine the control cell population and the nonspecific fluorescence. The results from flow cytometry were analyzed through Flowing Software 2.5.1. The cell recovery (CR) and yield of transfection (YT) were calculated as previously described [12]. Moreover, two combined transfection parameters were evaluated, which takes into account not only the percentage of cells expressing the protein (YT and $\%GFP^+$) but also the level of protein expression resultant from the microporation: $GFP\ MFI \times YT$ and $GFP\ MFI \times \%GFP^+cells$.

2.6.3. Plasmid copy number quantification

Plasmid DNA copy number quantification was carried out by StepOne™ Real-Time PCR detection system with Fast SYBR® Green Master Mix kit (Applied Biosystems). The reaction was performed by amplification of a 108 bp sequence within the GFP gene using GFP_pVX_Fwd (5' TCG AGC TGG ACG GCG ACG TAA A 3') and GFP_pVX_Rev primers (5' TGC CGG TGG TGC AGA TGA AC 3'). PCR reaction mixture consisted of 10µL of the 10X SYBR green mixtures, 1µL of each primer (0.25µM final concentration), 5µL containing of 10,000 MSC, and PCR-grade water to a final volume of 20µL. The thermal cycling program consisted of 10min at 95ºC, followed by 40 cycles of 15sec at 95ºC and 1min at 58ºC. A calibration curve of known amounts of plasmid was used to calibrate the RT-PCR system.

2.7. VEGF quantification

MSC culture supernatants were harvested on days 1, 4 and 7 and frozen at -80ºC until the analysis was performed. VEGF quantification was performed using RayBio® Human VEGF ELISA kit (RayBiotech), according to manufacturer instructions. Reagent and standard solutions preparation was performed according to kit protocol and samples were centrifuged to remove cells in suspension and diluted 1:1 in the Assay Diluent supplied. The standard curve was generated and the concentration of each sample was determined based on that calibration curve. The values were expressed as the mean of duplicates of one single experiment.

2.8. Data Analysis

With the exception of CHO experiments, all results are presented as mean± standard deviation of the mean (SEM).

3. Results and Discussion

3.1. *E.coli* BW2P *in vivo* recombination for Minicircle production

According to previous MC production from pMINI vector in *E.coli* BW2P, a recombination efficiency of nearly 100% was obtained when the induction with 0.01%(w/v) L-arabinose was performed in OD_{600nm} between 3.4 and 3.8 for one hour. These OD_{600nm} values correspond to late growth phase and it is advantageous because it allows the cell number and parental plasmids maximization before induction [19]. In a first approach, the previous strategy was replicated to pMINILi-CMV-VEGF production in *E.coli* BW2P. However, low recombination efficiencies were obtained (23.7%; 47.2%). Then, by increasing the induction time length to 5 hours, better recombination efficiencies were reached (81.7%, 89.9%). However, within fermentation and induction time, since MP contains the origin of replication, this species becomes predominant in plasmid population which is less desirable. A substantial decrease in recombination efficiency was already described when induction was performed closer to the stationary phase [19] and in this study this event was confirmed.

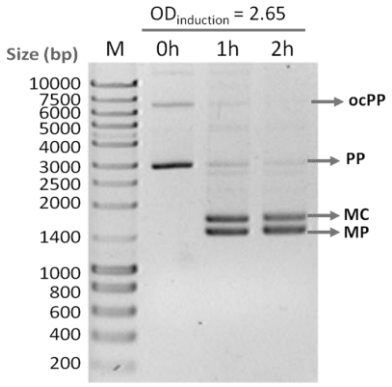

Figure 1 – Agarose gel electrophoresis of the produced and purified plasmid population of *E.coli* BW2P/ pMINILi-CMV-VEGF-GFP, using NZYTech Ladder III (Lane M), at the moment of induction (Lane 0h) and during 2 hours of recombination (Lanes 1h and 2h). The induction OD_{600nm} in this experiment was 2.65. The indicated MC, MP, PP and ocPP bands corresponds, respectively, to minicircle, miniplasmid, parental plasmid and open-circular parental plasmid and the unidentified bands are relaxed isoforms of MC, MP and PP.

Afterwards, by recombination induction at a lower OD_{600nm}, almost complete recombination was obtained after two hours of recombination (Figure 1). Using the knowledge behind the previous experiments results, all the *E.coli* BW2P strains, containing four different promoter plasmid constructions, were grown for MC production, according to the best conditions of induction established for *E.coli* BW2P/pMINILi-CMV-VEGF-GFP. The results of $OD_{induction}$ and the corresponding recombination efficiency from all the cell culture batches performed in 250 and 500mL are presented in Table 1. Recombinations efficiencies above 92% in all strains were observed when the culture is inducted with 0.01% (w/v) L-arabinose in a OD_{600nm} close to 2.5 (mid-late exponential growth phase). Moreover, there was not a significant difference in μ_{max} of the different genetically modified strains since their behavior during culture was very similar. According with the previous work developed in our laboratory (*E.coli* BW2P/pMINI, 1L bioreactor batch mode, Listner Complex medium [25], 20g/L and 40g/L of glycerol), μ_{max} of $0.56h^{-1}$ and $0.39h^{-1}$ were obtained[19]. These μ_{max} values are significantly lower to the ones obtained in present results, even using the same bacterial strain, because growth conditions were different and the glycerol is slowly metabolised by cells, minimizing metabolites production and thus enhancing plasmid production. Regarding other MC-producing strains, such as *E. coli* strain ZYCY10P3S2T harboring a PP of 7.06kbp [26], 10-fold higher μ_{max} values were obtained in present experiments, but the culture conditions, plasmid size and recombination system are clearly different.

3.2. Total pDNA purification

The volumetric yields obtained according to the manufacturer recommendations (4 purification columns for final OD_{600nm} (≈4.0) and culture volume (≤500mL)) were from 0.5 to 0.9mg pDNA/mL. Better volumetric yields were attained using only two purification columns, specifically around 1.5-fold more pDNA volumetric yield. Even just one experiment using 2 columns was performed for each construction, these experiments were

Table 1- Growth and recombination variables of different *E.coli* BW2P/pMINILi strains in 250 and 500mL LB medium.

Strain/pDNA	μ_{max} (h^{-1})		OD_{600nm} of Induction		Recombination Efficiency(%)	
	250mL	500mL	250mL	500mL	250mL	500mL
BW2P/pMINILi-CMV	0.95 ± 0.07	0.96*	2.56 ± 0.17	2.75*	96.44 ± 2.78	99.17*
BW2P/ pMINILi-hEf1a	1.03 ± 0.09	0.94 ± 0.08	2.49 ± 0.22	2.49 ± 0.14	98.65 ± 1.68	98.15 ± 1.07
BW2P/ pMINILi-mCMV+hEf1a (CpG free)	1.02 ± 0.09	1.00 ± 0.09	2.51 ± 0.13	2.46 ± 0.09	98.70 ± 1.32	98.46 ± 0.32
BW2P/ pMINILi-hEf1aCpG free	0.94 ± 0.06	0.91 ± 0.11	2.56 ± 0.15	2.53 ± 0.21	92.68 ± 4.27	96.37 ±1.59

*Only one growth experiment was performed.

accomplished in different days, and therefore reproducibility is present. Moreover, quality of purified pDNA was not altered. Yields of constructions with CMV and hEf1α promoters and mCMV+hEf1α and hEf1α CpG free promoters were similar among them, respectively. BW2P/pMINILi-hEf1α CpG free was the strain that produced a higher volumetric yield (0.88±0.09 and 1.77mg pDNA/L). Size has a crucial influence on DNA yield and this PP is around 500bp smaller than the others, thus its replication within culture should be more pronounced (high number of pDNA copies). In previous work, 2.9 ± 0.5 mg pDNA/L was achieved using a 50mL (LB medium) shake flask system with BW2P/pMINI after 4.5hours of incubation [19]. Since the final OD_{600nm} was not specified in the previous study, no real comparison with the present results can be done. Even so, since the strains are the same and the pMINILi plasmids are derivatives of pMINI, one possible explanation for the differences is based on the purification methods used. MN purification procedure is more stringent in order to obtain a high quality and endotoxin free pDNA sample, thus a lower pDNA recovery can be observed in comparison with High Pure Plasmid Isolation Kit protocol (Roche).

3.3. Minicircle purification

3.3.1. Anion Exchange Chromatography (AEC)

AEC requires, as a first and functional step in this process, a PvuII enzymatic digestion of recombined and purified pDNA sample that originated short linear fragments (337-414bp) from MP and unrecombined PP and the undigested supercoiled and relaxed MC (pMINILi and its derivative constructions contain six PvuII restriction sites). Based on reversible exchange of anions in solution with anions groups of the molecules electrostatically bound to the support media, the CIM®-DEAE Disk was successfully implemented as intermediate step of the GMP pDNA manufacturing process in previous studies [27]. In this process, the first linear gradient separation (20-80%B) of the digested recombination products, performed in all CIM®-DEAE purification experiments, was used to define the salt concentrations required for elution of the different DNA species in the mixture, during the step gradient chromatography. For all PvuII digested plasmid constructs, in the chromatogram (Figure 2), a first set of peaks was observed, which included all molecules that have a low interaction with column, including protein PvuII used for enzymatic digestion[19], and eluted in the flow through. During linear gradient performance, two main peaks were present and according to the previous developed work in our laboratory [19], the first broad peak corresponded to the short linear fragments which have a lower negative charge density in comparison with the supercoiled and relaxed MC minicircle that were released in the second sharper peak (Figure 2). Moreover, the resolution of the two different groups of DNA molecules in these conditions was enough to comfortably design a step gradient. In the step-gradient chromatography, the first long elution step with a lower salt concentration allowed the impurities elution, appearing as a first peak in the chromatogram (Figure 3A). Then, a sharper peak, during the elution step at a higher salt concentration, appeared. At the end of the run, the final step of 100%B was applied to regenerate the column, eluting the remaining impurities from the column. The gel electrophoresis of some peak fractions confirmed that the first peak consisted mainly in short linear fragments, having also some MC and the second peak was constituted by supercoiled and relaxed MC (Figure 3B). The results from this step-gradient purification proved the ability of this method application for separation of impurities from MC.

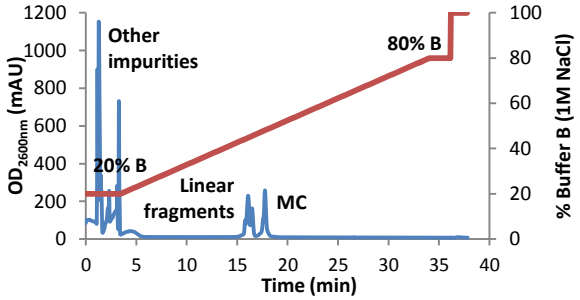

Figure 2 - Chromatographic separation of pMINILi-CMV-VEGF-GFP recombined and digested products on a CIM®-DEAE disk using a linear gradient between 20% and 80% 1M NaCl.

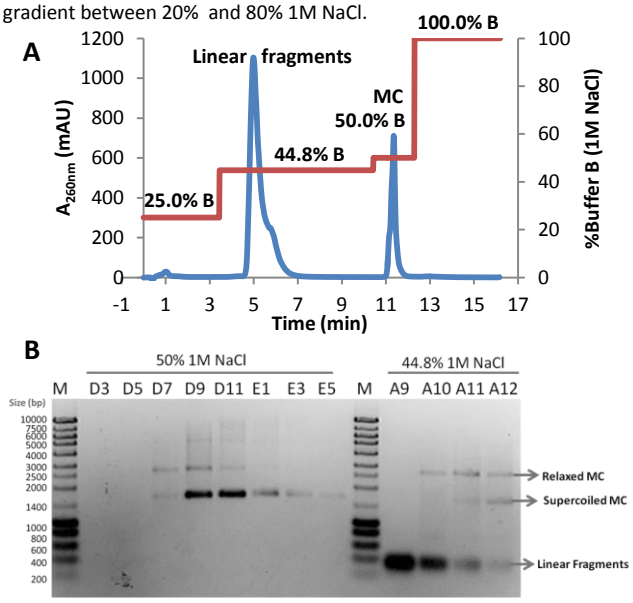

Figure 3 – Chromatographic separation of pMINILi-CMV-VEGF-GFP recombined and digested products on a CIM®-DEAE disk using a step gradient **(A)** and corresponding peak fractions are visualized on electrophoretic gel **(B).**

Moreover, in MC fractions, the supercoiled conformation was presented at higher quantity in comparison with the relaxed conformation, which is desirable to allow better efficiencies in transfection experiments [27-29]. However, the salt concentration required to elute the DNA impurities could vary depending on the sample (concentration and charge density differences) and buffer batches or on environmental factors which influence the conductivity, such as temperature. Therefore, an optimized protocol was tested because contamination of MC peak fractions with linear fragments occurred in more than one purification experiment. By the addition of one step that corresponds to the second step in the method and to the salt concentration of the top of linear fragments peak in linear gradient, it was possible to eliminate most of the linear fragments present in the loaded sample and if the elution conditions would not be enough to discard all linear fragments, the next step could be used for that purpose. There were some experiments where this additional step allowed the non-contamination of MC peak fractions, because all linear fragments eluted before the step of MC elution, and in most of them, this additional step was sufficient to elute all impurities and the next two step peak fractions were composed only by pure MC. There is the possibility of the used CIM-DEAE disk is damaged and not fully functional (resolution, binding capacity and back pressure affected) due to recurrent use and regeneration of column for purification of MC and other biomolecules that led to progressive degradation of functional groups [30]. However, the optimized method allowed better recovery of MC pure fractions, once at least one step had pure MC fractions, which could not be accomplished in the previous method if the salt concentrations of the two steps were not well set.

3.3.2. Hydrophobic Interaction Chromatography (HIC)

Before HIC, the Nb.BbvCI enzymatic digestion was the crucial step to differentiate MC from MP and PP. Typically pDNA molecules present hydrophilic nature since the majority of the bases are shielded inside the double helix. In the presence of high concentrations of a kosmotropic salt, the hydrophobicity of SC MC isoform increases as a consequence of the underwinding (negative supercoiling). On the other hand, nicked and relaxed MP and PP present a lower hydrophobic profile than MC isoforms [31, 32]. Using a negative HIC strategy, during the chromatographic step, bound biomolecules, including MC and nicked MP and PP, are eluted by reducing the hydrophobic interaction and in this particular method, hydrophobic interactions were weakened by reducing the concentration of ammonium sulphate in the mobile phase. According to the previous pDNA purifications using HIC [31,32], some adjustments and optimizations in salt concentrations were implemented and by a step gradient method, MC isolation was possible. The first peak (17%B) was relative to relaxed forms of MP and PP, the second one was composed by relaxed and supercoiled forms of MC (35%B) and at 100%B, the remaining bound macromolecules were eluted (Figure 4B). For all recombined, purified and digested pMINILi constructions, the same HIC method was applied and the reproducibility of HIC for MC purification in these conditions was proved (Figure 4A).

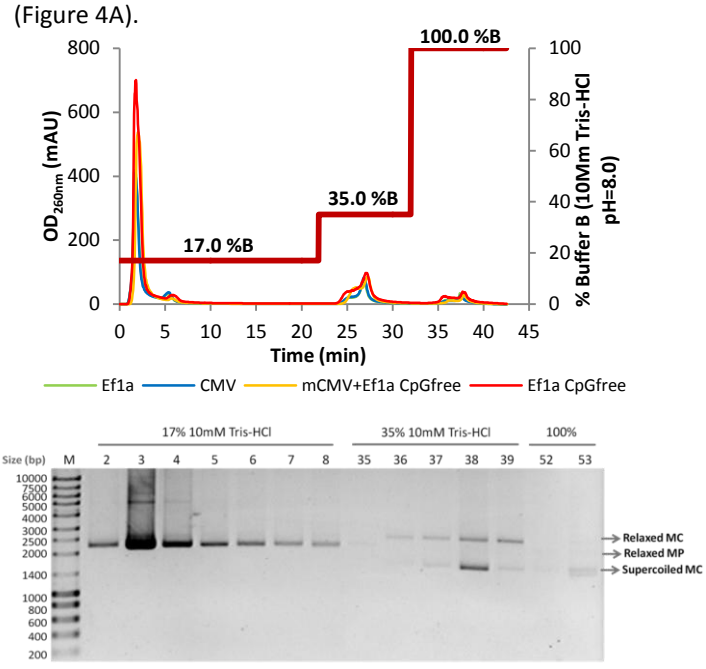

Figure 4–Chromatographic separation of pMINILi recombined and Nb.BbvCI DNA nickase digested products on a PheFF-HS resin using a step gradient (A); pMINILi-CMV-VEGF-GFP derived MP and MC corresponding peak fractions visualized on electrophoretic gel (B).

Regarding the percentage of MC in recombined, purified and digested samples, CIM-DEAE purifications revealed that MC occupied 14.69 ± 1.60% of the loaded sample and in HIC, this percentage was 16.50 ± 1.69%. Despite differences were not significant, it is important to notice that in CIM-DEAE purifications, some MC eluted during the steps of linear fragments elution, therefore a portion of MC was lost during this phase. The MC recovery mean values using CIM-DEAE monolith were similar and higher (50.8 ± 8.9 - 67.4 ± 17.4%) than the ones obtained with HIC purifications (40.5 - 45.6%). However, if independent yields of the same MC purification experiments are analyzed, meaningful discrepancies are observed. These differences were also observed before, during the

development of this CIM-DEAE purification method: values from 56.9 to 94.4% for MC recovery were obtained [19]. Despite the low average MC recoveries from AEC in the present study, these results demonstrate the possible variability of this method according to the sample load and established method. Since only one HIC experiment to each MC was performed and higher mass load was applied, no evident conclusion can be accomplished about which is the best method for MC purification.

3.3.3. Minicircle confirmation

All MC were confirmed by enzymatic digestion (Figure 5). In the DNA sequencing results, one point mutation was detected in the GFP gene sequence (G→A) that led to an exchange of an arginine by a histidine. Since these aminoacids belong to the same group, which is aminoacids with positively charged R group, no negative consequences for GFP protein structure and activity were admitted.

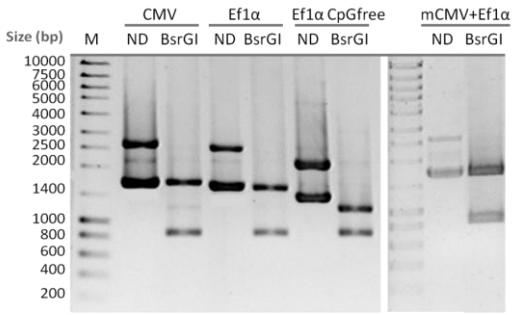

Figure 5 - BsrGI digestion of MC after all purification downstream processing: NZYTech Ladder III (Lane M); Non-digested MC (Lanes ND) and BsrGI digested MC (Lanes BsrGI) relative to the four promoters: MC CMV (1618bp+839bp), MC hEf1α (1531bp+839bp), MC mCMV+hEf1α CpG free(1618bp+839bp) and MC hEf1α CpG free (1180bp+839bp).

3.4. BM MSC Microporation

3.4.1. Flow cytometry analysis

Regarding cell viabilities values, there were no significant differences between each vector neither with control cells and the values were all above 90% during 7days of experiment. In both CHO cells and MSC transfections, the presence of vectors inside cells showed do not cause significant damages over time unless during their entrance to the cell where it was observed significant decrease of alive cells after transfection, measured by cell recovery and yield of transfection values. In CHO cells transfections, by fluorescence microscopy, obvious green fluorescence from GFP expression in all vectors, PP and MC, was observed. Moreover, MC revealed predominantly better results in comparison with the respective PP. On the other hand, in MSC cell transfections the same fluorescence was not clearly identified until flow cytometry was realized to obtain values of this expression. Taking into account GFP mean intensity and yield of transfection (Figure 6), MSC transfected with MC CMV showed the highest value, followed by MSC pVAX-VEGF-GFP and excluding MSC pVAX-GFP from this analysis. Both vector results, regarding this product value, had a relevant SEM value that shows the need to carry out further experiments in order to conclude if the GFP expression differences of these vectors are significant or not. Contrary, MC mCMV+hEF1α transfected MSC product result was lower than pVAX-VEGF-GFP and MC CMV but presented a higher level of confidence since SEM value was lower. Considering GFP mean intensity and GFP-expressing transfected MSC product (Figure 7), MSC pVAX-VEGF-GFP showed an initial higher value but on day 4 it approached to the one from MC CMV, which supports the larger drop of pVAX-VEGF-GFP GFP expression in comparison with MC CMV.

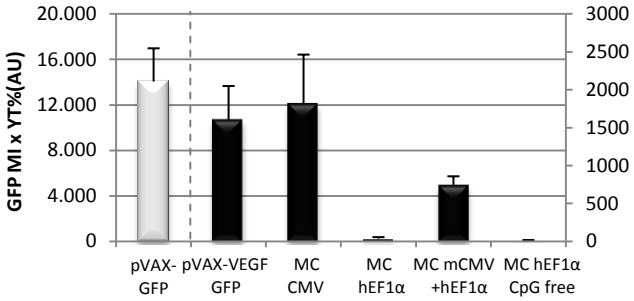

Figure 6 - GFP expression mean intensity and yield of transfection product values of MSC transfection experiments with pVAX-GFP, pVAX-VEGF-GFP and VEGF-GFP encoding MC. Cell data obtained from three independent experiments (n=3) 24h after transfection. Values are presented as mean ± SEM and the dashed line separates the pVAX-GFP from the remaining vector values scale.

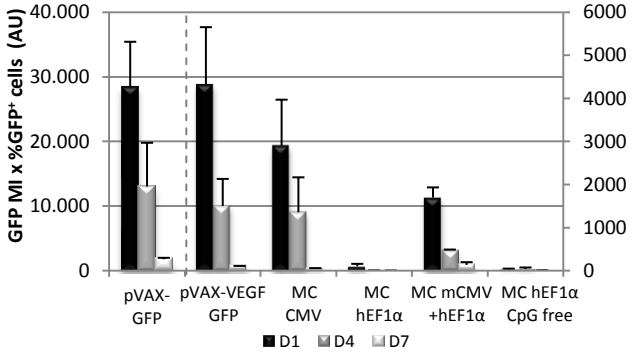

Figure 7 - GFP expression mean intensity and GFP^+ percentage product values of MSC transfection experiments with pVAX-GFP, pVAX-VEGF-GFP and VEGF-GFP encoding MC. Cell data obtained from three independent experiments (n=3) 1, 4 and 7 days of cell culture after transfection. Values are presented as mean ± SEM and the dashed line separates the pVAX-GFP from the remaining vector values scale.

MSC MC mCMV+hEF1α showed a lower but more constant decrease rate in GFP expression. On day 7, independently of the vector, insignificant values of GFP expression were reached relatively to the initial ones. The MSC pVAX-GFP results were in general supported by literature [12]. The higher variable values in comparison with MSC transfected with VEGF-GFP-containing vectors should be explained by the higher transcription rate for GFP gene and consequently the higher number of GFP mRNA transcripts and protein. On the other hand, no successful results were obtained for MSC MC hEF1α and MC hEF1α CpG free due to their significant low values of MSC transfection parameters and also GFP expression. As a result, no more experiments were perfomed with these vectors. Fluorescence and bright field images were taken and GFP fluorescence intensity decrease over time for all vectors was observed (Figure 8). MSC MC hEf1α and hEf1α CpG free are not showed since fluorescent cells were difficult to record.

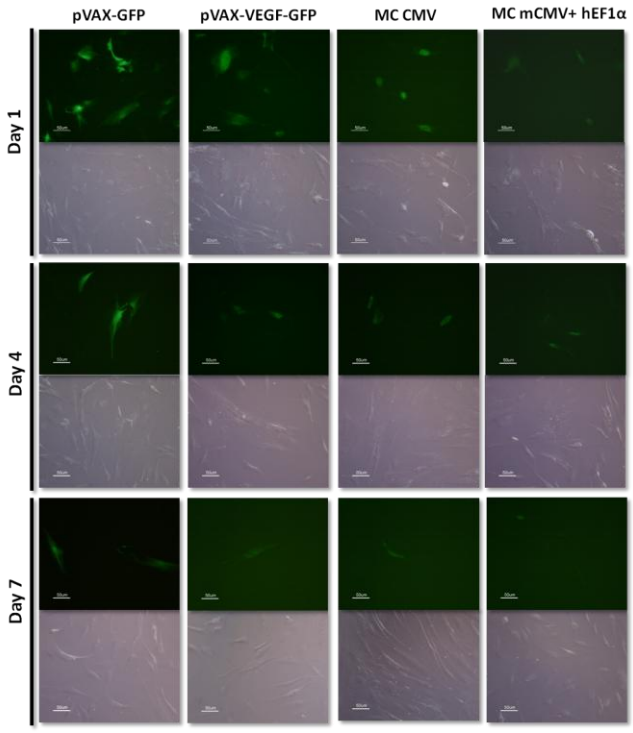

Figure 8-Fluorescence and bright field microscopic images of transfected MSC with pVAX-GFP, pVAX-VEGF-GFP, MC CMV and MC mCMV+hEF1α CpG free 1, 4 and 7 days after microporation experiment.

4.1.1. Plasmid Copy Number Quantification

Analyzing RT-PCR results (Table 2), different values and relations from the ones obtained were expected. Firstly, it is important to note that since the cells continue to divide after the transfection procedure, reduction in PCN/cell should be observed and attributed to vector distribution between daughter cells, since it do not replicate, and also to degradation [7]. In this study, with exception of the pVAX-VEGF results that demonstrated the decrease in PCN/cell over time, the other vector results showed a significantly higher value of PCN on day 4. As a matter of fact, cell counting on day 1 was much more prone to errors that on day 4 wherein the cell number is larger. Therefore, samples from day 1 could have less than 10,000 MSC. Moreover, the supernatant aspiration could drag out a considerable number of cells. Besides this unanticipated result, more discordance was observed. In the literature, the entrance of a higher number of MC molecules into the cells comparatively with pDNA was several times reported [33-36] and associated to the greater efficiency of MC in gene expression. Our results showed a completely discordant relation. pDNA transfected MSC gave higher PCN/cell than MC MSC. Additionally, when RT-PCR results were compared with the percentage of transfected cells assessed by flow cytometry analysis, no proportionality was obtained. MC CMV and mCMV+hEF1α CpG free flow cytometric results were comparable and sometimes even better than the pVAX-VEGF-GFP and the PCN/cell values did not demonstrate that correspondence. Another matter of discussion is the overall low number of PCN/cell for both type of vectors, but mainly for MC, once the theoretical value of PCN/cell before transfection is $1.7x10^6$ vectors per cell ($2.5x10^{11}$ molecules were added to each $1.5x10^5$ MSC).

Table 2 – Plasmid copy number per cell of pVAX-GFP, pVAX-VEGF-GFP, MC CMV and MC mCMV+hEF1α CpG free transfection experiments. Values are presented as mean ± SEM of two independent MSC transfection experiments.

Vector		PCN/cell
pVAX-GFP	D1	722 ± 467
	D4	4408 ± 1537
	D7	486 ± 314
pVAX-VEGF	D1	4315 ± 975
	D4	605 ± 165
	D7	118 ± 78
MC CMV	D1	6 ± 3
	D4	247 ± 172
	D7	5 ± 3
MC mCMV+ hEf1α CpG free	D1	7 ± 5
	D4	143 ± 95
	D7	43 ± 2

4.1.2. VEGF Quantification

During 7 days, the non-transfected and transfected MSC media was not changed, thus an increased VEGF concentration in the supernatants over time was expected (Figure 9). Both pVAX-VEGF-GFP and MC modified MSC produced more VEGF comparatively to non-transfected MSC. On day 1, VEGF concentration of MC CMV transfected cells presented an approximately 8-fold increase in relation to control cells, whereas MC mCMV+hEF1α CpG free and pVAX-VEGF-GFP presented just about 3 and 2-fold increase, respectively (Figure 9). On day 4 and comparatively to day 1, control cells produced 5.3 times more VEGF and pVAX-VEGF-GFP, MC CMV and MC mCMV+hEF1α CpG free expressed 11.3, 4.2 and 11.9 times more VEGF, respectively. Relatively to control cells, MC CMV transfected MSC attained the highest concentration with 6.1-fold increase, immediately followed by the 5.9-fold increase from MC mCMV+hEF1α CpG free (Figure 9). On day 7, the VEGF concentrations in all transfected MSC were 3.4 (pVAX-VEGF-GFP), 4.9 (MC CMV) and 4.6 (MC mCMV+hEF1α CpG free) times superior than the concentration from control cells and from day 4, their increase was not more than twice. At the end, MC CMV presented the highest VEGF concentration (23 812 pg/mL), followed by MC mCMV+hEF1α CpG free (22 514 pg/mL) and then pVAX-VEGF-GFP (16 641 pg/mL). VEGF production in MSC transfected with MC was at least 1.3-fold higher than pVAX-VEGF-GFP modified MSC.

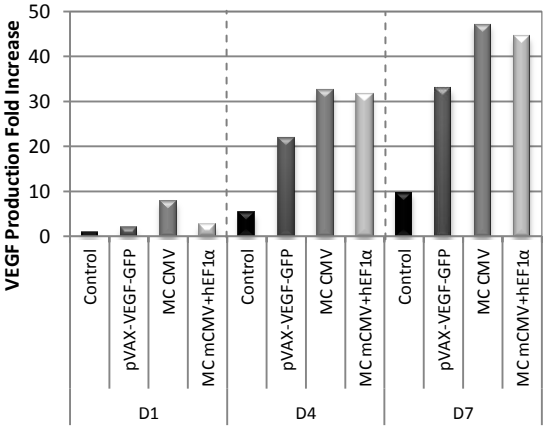

Figure 9 - Human VEGF Cumulative Fold Increase on days 1, 4 and 7 after MSC transfection with pVAX-VEGF-GFP, MC CMV and MC mCMV+hEF1α CpG free. Non-transfected MSC were analyzed as control cells and values are presented as mean of the duplicates from one single experiment ± SEM.

These concentration values were superior to the one obtained using MC-CMV-VEGF in BM MSC [33] and similar to what was obtained with a MC-CMV-VEGF transfection in C2C12 skeletal muscle cell line [37]. However it is desirable, because supernatant samples were not centrifuged before freezing at -80ºC, these concentrations can be overestimated due to release of the intracellular VEGF-GFP protein content to the media. On the other hand, since alive MSC were attached to the well surface, only death cells were collected in supernatants and their VEGF-GFP content can be considered negligible.

5. Conclusion and future perspectives

The VEGF-encoding MC production by the process developed in our laboratory and BM MSC microporation with these MC in order to overexpress VEGF in a sustained and transient manner were the main goals of this master thesis. To achieve these aims, some successful optimizations and alternative procedures were tested and introduced, particularly in the MC production technology. According to the previous knowledge [19] and the *E.coli* BW2P/pMINILi constructions growth, it is possible to conclude that the recombination efficiency in this system is highly dependent on the induction growth phase. Higher recombination efficiencies were achieved when the L-arabinose induction was performed in the period between mid-late exponential phase and before the stationary phase. From now on, since medium composition and other factors can influence the growth, before any recombination induction, a growth curve of this strain transformed with different PP should be performed to identify the best induction conditions. On the other hand, since MC mass produced using batch system with LB medium is considerably low for the proposed therapeutic approach, an optimization process is a crucial requirement. A recent study reported a 2.21-fold increase in MC production by optimization of key parameters such as growth temperature, inductor concentration and recovery time [26]. Concerning chromatographic methods used for MC purification, MC recoveries from both methods must be improved once significant quantities of MC were lost during these purification procedures. HIC strategy showed to be superior for our purpose in terms of quality of final MC, although it was not better regarding MC recovery values. Since CIM-DEAE monolithic chromatography is described in the literature as a better method than resin based purifications, besides the MC recovery increase need, its further optimization is required in order to eliminate high molecular weight smear that appeared in MC peak fractions and also to eliminate bacterial contaminations in MSC transfection experiments, if it happen again. Finally, the analysis of all the results and discussion from cell

counting and viability, flow cytometry, RT-PCR and ELISA, showed that produced MC are clearly biological active molecules and MSC are less favorable to genetic manipulation than CHO cells. Moreover, no clear conclusions can be accomplished about the enhanced VEGF-GFP expression of MSC transfected with MC molecules. MC hEf1α and hEf1α CpG free proved to be inadequate vectors for the goal of this genetic and cellular therapy. Nevertheless, there was more than one evidence that VEGF-GFP encoding MC with CMV and mCMV+hEF1α CpG free promoters could provide at least a similar VEGF expression when compared to pVAX-VEGF-GFP. Alternatively to VEGF, other target genes can be study to treat CVD [38].

6. References

1. Global status report on noncommunicable diseases 2010. Edited by Alwan A. Genebra: World Health Organization; 2011.
2. Yang F. *et al*. *Proc Natl Acad Sci U S A* 2010, **107**(8):3317-22.
3. Hwang N.S. *et al*. *Tissue Eng* 2006, **12**(9):2695-706.
4. Uccelli A. *et al*. *Nat Rev Immunol* 2008, **8**(9):726-36.
5. Browne C.M. *et al*. The Biology of Mesenchymal Stem Cells in Health and Disease and Its Relevance to MSC-Based Cell Delivery Therapies. In: *Mesenchymal Stem Cell Therapy*. Edited by Chase LG, Vemuri MC. New York: Springer; 2013: 63-86.
6. Pons J. *et al*. *J Gene Med* 2009, **11**(9):743-53.
7. Azzoni A.R. *et al*. *J Gene Med* 2007, **9**(5):392-402.
8. Myers T.J. *et al*. *Expert Opin Biol Ther* 2010, **10**(12):1663-79.
9. Ginn S.L. *et al*. *J Gene Med* 2013, **15**(2):65-77.
10. Madeira C. *et al*. *J Biomed Biotechnol* 2010, **2010**:735349.
11. Boura J.S. *et al*. *Hum Gene Ther Methods* 2013, **24**(1):38-48.
12. Madeira C. *et al*. *J Biotechnol* 2011, **151**(1):130-6.
13. Lim J.Y. *et al*. *BMC Biotechnol* 2010, **10**:38.
14. Nowakowski A. *et al*. *Acta Neurobiol Exp* 2013, **73**(1):1-18.
15. Mayrhofer P. *et al*. *Methods Mol Biol* 2009, **542**:87-104.
16. Argyros O. *et al*. *J Mol Med (Berl)* 2011, **89**(5):515-29.
17. Chen Z.Y. *et al*. *Mol Ther* 2003, **8**(3):495-500.
18. Chen Z.Y. *et al*. *Hum Gene Ther* 2005, **16**(1):126-31.
19. Simcikova M. Development of a process for the production and purification of minicircles for biopharmaceutical applications. Lisboa: Universidade de Lisboa; 2013.
20. Kobelt D. *et al*. *Mol Biotechnol* 2013, **53**(1):80-9.
21. Grund M. *et al*. Minicircle Patents: A Short IP Overview of Optimizing Nonviral DNA Vectors. In: *Minicircle and Miniplasmid DNA Vectors: The Future of Non-viral and Viral Gene Transfer.* Edited by Schleef M, First Edition: Wiley-VCH Verlag GmbH & Co. KGaA; 2013: 1-6.
22. Mayrhofer P. *et al*. *J Gene Med* 2008, **10**(11):1253-69.
23. Alves C. Development of a method for the purification of minicircles. Lisboa: Universidade de Lisboa; 2014.
24. Simcikova M. *et al*. *Vaccine* 2014, **32**(24):2843-6.
25. Listner K. *et al*. *Methods Mol Med* 2006, **127**:295-309.
26. Gaspar V.M. *et al*. *Hum Gene Ther Methods* 2014, **25**(2):93-105.
27. Urthaler J. *et al*. *J Chromatogr A* 2005, **1065**(1):93-106.
28. Prazeres D.M.F. *et al*. *Chemical Engineering and Processing: Process Intensification* 2004, **43**(5):609-24.
29. Remaut K. *et al*. *J Control Release* 2006, **115**(3):335-43.
30. CIM® Disk Monolithic Column Instruction Manual (BIA Separations)
31. Freitas S.S. *et al*. *Separation and Purification Technology* 2009, **65**(1):95-104.
32. Pereira L.R. *et al*. *J Sep Sci* 2010, **33**(9):1175-84.
33. Pereira T. Non-viral engineered human mesenchymal stem/stromal cells to promote angiogenesis. Lisboa: Universidade de Lisboa; 2013.
34. Ribeiro S. *et al*. *Cell Reprogram* 2012, **14**(2):130-7.
35. Chabot S. *et al*. *Gene Ther* 2013, **20**(1):62-8.
36. Madeira C. *et al*. *Biomacromolecules* 2013, **14**(5):1379-87.
37. Chang C.W. *et al*. *J Control Release* 2008, **125**(2):155-63.
38. Kanashiro-Takeuchi R.M. *et al*. *Proc Natl Acad Sci US A* 2012, **109**(2):559-63.